PETROLEUM EXPLORATION AND DEVELOPMENT
Volume 47, Issue 6, December 2020
Online English edition of the Chinese language journal

Available online at www.sciencedirect.com
ScienceDirect

Cite this article as: PETROL. EXPLOR. DEVELOP., 2020, 47(6): 1246–1261.

RESEARCH PAPER

Eogenetic karst and its control on reservoirs in the Ordovician Majiagou Formation, eastern Sulige gas field, Ordos Basin, NW China

XIE Kang[1, 2], TAN Xiucheng[1, 2,*], FENG Min[3], WANG Baobao[1, 2], ZHONG Shoukang[1, 2], YANG Mengying[1, 2], NIE Wancai[1, 4], QIAO Zhanfeng[5], ZENG Wei[2]

1. State Key Laboratory of Oil and Gas Reservoir Geology and Exploitation, Southwest Petroleum University, Chengdu 610500, China;
2. Department of Key Laboratory of Carbonate Reservoir of CNPC, Southwest Petroleum University, Chengdu 610500, China;
3. Exploration and Development Research Institute of PetroChina Changqing Oilfield Company, Xi'an 710018, China;
4. Yihuang Natural Gas Department of PetroChina Changqing Oilfield Company, Xi'an 710018, China;
5. PetroChina Hangzhou Research Institute of Geology, Hangzhou 310023, China

Abstract: To further ascertain the origin of the Ordovician Majiagou Formation reservoirs in the Ordos Basin, the M_5^4-M_5^1 sub-members of the Ordovician Majiagou Formation in the eastern Sulige gasfield of Ordos Basin were taken as examples to analyze the vertical development characteristics of eogenetic karst and to discover the dissolution mechanism and its control on reservoirs through observation of a large number of cores and thin sections. According to detailed analysis of petrologic characteristics, the reservoir rock types include micritic dolomite, grain dolomite and microbialite which have mainly moldic pore, intergranular (dissolved) pore, and (dissolved) residual framework pore as main reservoir space respectively. The study area developed upward-shallowing sequences, with an exposure surface at the top of a single upward-shallowing sequence. The karst systems under the exposure surface had typical exposure characteristics of early dissolution and filling, indicating these reservoirs were related to the facies-controlled eogenetic karstification. With the increase of karstification intensity, the reservoirs became worse in physical properties.

Key words: porous reservoir; reservoir characteristics; eogenetic karst; dolomite; Majiagou Formation; Ordovician; Sulige gas field; Ordos Basin

Introduction

Experiencing the long and strong superposition reformation of weathering crust karst from Caledonian to early Hercynian for 130 Ma[1], the carbonate rocks of the Ordovician Majiagou Formation in Ordos Basin are complex in lithology and lithofacies, so it is difficult to tell the initial force driving the formation of the pore-type reservoirs there, which restricts the prediction and evaluation of this type of reservoir. Most of the previous studies concluded that the carbonate reservoirs in the M_5^4-M_5^1 sub-members of the Majiagou Formation were weathering crust karst-type reservoir formed by the overall uplift and long-term exposure of the basin caused by the Caledonian - early Hercynian tectonic movement[2–3]. But for the genesis of the dolomite reservoirs with moldic pores, the main body of the pore-type reservoir in the M_5^4-M_5^1 sub-members, there are three viewpoints: (1) This kind of reservoir was formed by weathering crust karst in the Caledonian - early Hercynian period[3–4]; (2) The reservoir space is the product of anhydrite nodule dissolution during the high frequency exposure in penecontemporaneous period and the weathering crust karst of the Caledonian - early Hercynian period[5]; (3) This kind of reservoir is the result of high-frequency exposure karst in the syngenetic - eogenetic period, and is controlled by lithology and lithofacies jointly[6–7]. These opinions have not fully explained from the combination of macroscopic sequence combination and microscopic characteristics. In view of this, based on abundant core and thin section data of the M_5^4-M_5^1 sub-members in the eastern part of the Sulige gas field, the macroscopic sequence and microscopic characteristics of the

Received date: 05 Mar. 2020; **Revised date:** 05 Nov. 2020.
*** Corresponding author.** E-mail: tanxiucheng70@163.com
Foundation item: Supported by the China National Science and Technology Major Project (2016ZX05004006-001-002); CNPC-Southwest Petroleum University Innovation Consortium Technology Cooperation Project.
https://doi.org/10.1016/S1876-3804(20)60133-7
Copyright © 2020, Research Institute of Petroleum Exploration & Development, PetroChina. Publishing Services provided by Elsevier B.V. on behalf of KeAi Communications Co., Ltd. This is an open access article under the CC BY-NC-ND license (http://creativecommons.org/licenses/by-nc-nd/4.0/).

reservoir rocks (including micrite dolomite with moldic pore, grain dolomite and microbialite) have been examined closely to make clear the relationship between exposure in the early diagenetic period driven by high-frequency sea level fluctuations and the reservoir development, the controlling effect of the early diagenetic karst on reservoirs, and the petroleum geological significance of the later weathering crust karst. We hope that the research results can provide theoretical support for prediction of this kind of reservoirs, and provide new materials for the theory of karst geology in the early diagenesis period.

1. Geologic setting

Ordos Basin, located in the western margin of north China platform, with an area of about 2.5×10^5 km^2, is one of the major oil-bearing basins in western China. According to the tectonic characteristics of Mesozoic, the basin can be divided into six first-order tectonic units, namely, the northern Yimeng uplift, the central Yishaan slope, the eastern Jinxi fault-fold belt, the southern Weibei uplift, the Tianhuan depression and the western margin fault-fold belt to the west[8–9]. The study area is the northeast area of Sulige gas field, with the main part located in the Yishaan slope (Fig. 1).

During the sedimentary period of M_5 Member of the Middle Ordovician Majiagou Formation, on the one hand, the basement of the Ordos Basin rose and sea level fell; on the other hand, due to the arid and hot climate of the basin, the

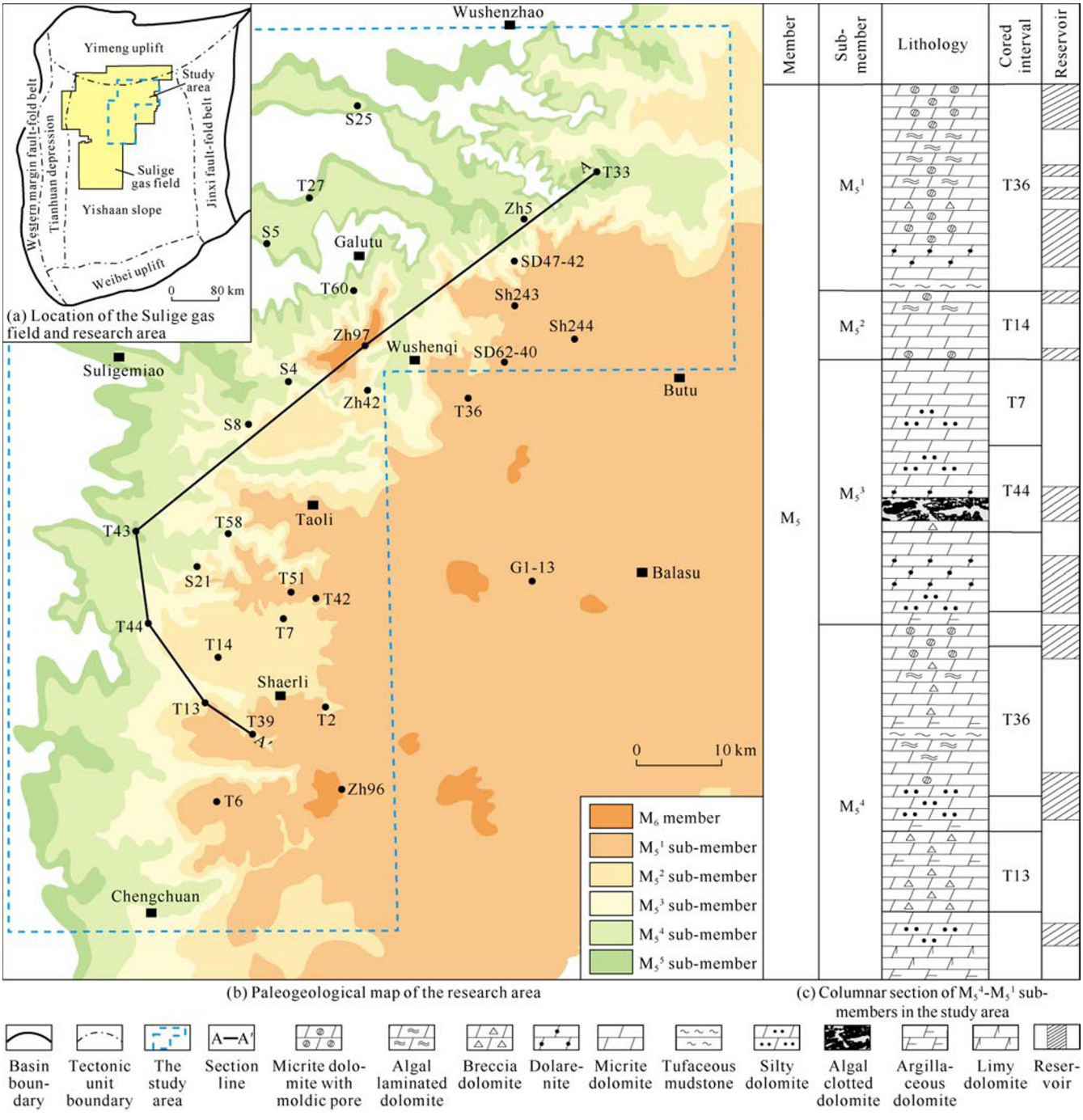

Fig. 1. Location and geological setting of the study area.

large evaporation led to constant increase of seawater salinity in the basin, and the turn-up of limited-evaporative platform environment. The M_5 Member is mainly composed of micrite dolomite, grain dolomite and microbialite [4–5,8] (Fig. 1c).

At the end of Ordovician, the North China Platform uplifted overall due to the Caledonian movement and suffered about 130 Ma of weathering erosion, causing the missing of Upper Ordovician–Lower Carboniferous in the main part of the platform [1, 3]. The Middle Ordovician Majiagou Formation experienced long time dissolution in multiple stages, so the Ma6 Member at the top of Majiagou Formation remains only sporadically in the study area. The M_5^4 to M_5^1 sub-members are also eroded to various degrees. The micrite dolomite with moldic pore, grain dolomite and microbialite are the main reservoir rocks in the Lower Paleozoic of Ordos Basin now (Fig. 1b).

2. Reservoir rocks and sequences

Rock types and sequence combinations are the basis for analyzing sea level fluctuations and judging the presence of exposure driven by early high-frequency sea level changes. Based on abundant core and thin sections data of the M_5^4-M_5^1 sub-member in the eastern part of Sulige gas field, we found that the study area has three primary types of carbonate rocks, micrite dolomite, grain dolomite and microbialite (Fig s. 2 and 3), followed by medium-fine crystal dolomite and karst breccia secondarily. These rocks constitute four kinds of upward shallowing sequences vertically, indicating that exposure karst related to high frequency regression might occur in the area. The characteristics of each rock type are described below.

2.1. Main types of the reservoir rocks

2.1.1. Micrite dolomites

2.1.1.1. Micrite dolomite

Micrite dolomite is commonly seen in M_5^4-M_5^1 sub-members, and often brownish gray to gray, with massive bedding, horizontal bedding, rhythmic bedding, etc. The massive bedding dolomite is relatively homogeneous, with biological burrows occasionally seen. The laminar micrite dolomite is composed of thin interbedded argillaceous micrite dolomite and bright silty dolomite (Fig. 3a, 3e). This kind of rock has no obvious pores in the core (Fig. 3a), but when karst develops, may have intercrystalline dissolution micropores, especially dominant karst channels such as karst fissures and karrens well-developed (Fig. 3f).

2.1.1.2. Micrite dolomite with moldic pore

This type of dolomite is widespread in the M_5^4-M_5^1 sub-members of the study area, and is the most important reservoir rock in the study area (Fig. 1c). It is characterized by the development of a variety of moldic pores formed by selective dissolution, mainly including gypsum and salt moldic pores which are formed by selective dissolution of evaporate

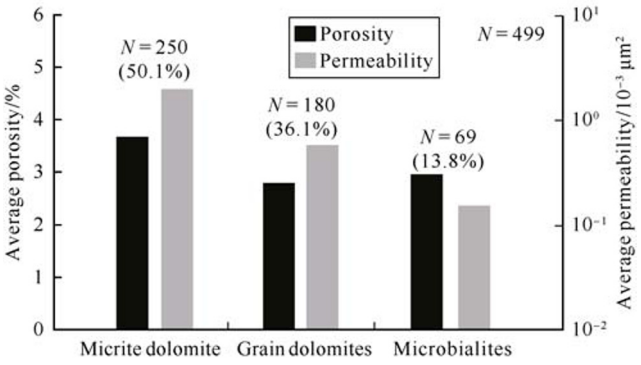

Fig. 2. Histograms of average porosity and permeability of major reservoir rocks in the study area (*N*—number of sample).

minerals. Macroscopically, the micrite dolomite with moldic pore is mostly brown-gray and massive, with moldic pores dispersed in it (Fig. 3c). The moldic pores are generally about 2 mm in size (Fig. 3g), and mostly in near circular shape, secondarily in plate shape. The moldic pores were speculated as the product of anhydrite nodule dissolution before[6]. But on thin sections, the moldic pores are mostly in rounded polygon shape, or in square shape when the dissolution rounding is not obvious. This suggests that they were more likely to be crystals of evaporite before dissolving, possibly halite. It may be more appropriate to call them salt-moldic pore. The moldic pores are filled or partially filled with calcite, dolomite, quartz (Fig. 3g), and seepage sand (Fig. 3g, 3h). Although this type of reservoir space is commonly known as "gypsum" moldic pore, in fact the moldic pore only defines the three-dimensional shape of the reservoir space, which is mainly composed of filling residual pores, micropores between seepage sand grains and intercrystalline dissolution micropores (Fig. 3h).

2.1.2. Grain dolomites

Grain dolomites in the M_5^4-M_5^1 sub-members of the Majiagou Formation in the study area appear in high frequency. According to the grain composition, they can be divided into (gravel-bearing) dolarenite and oolitic dolomite (Fig. 3i–3m). Sparry grain dolomite was generally formed in the high- energy zone above the wave base. Due to strong water energy, sediments were washed relatively clean, and the sparry grain dolomite with intergranular pores is another major type of reservoir rock in the region after reformed by karst.

2.1.2.1. Gravel-bearing dolarenite

The dolarenite is usually gray-grey-brown, massive, with a grain content of 60% to 80%, a grain size of 0.2 to 1.0 mm, and gravel grains larger than 2 mm usually accounting for less than 10%. The grains are good in sorting and rounding, mostly in sub-round to round shapes, in point-line contact (Fig. 3i), and supported by grains. The grains are composed of micrite dolomite. When the recrystallization is strong, the original rock fabric is destroyed, thus forming the powder crystal dolomite (with grain shadow) (Fig. 3j). This type of reservoir rock is characterized by the development of intergranular (dis-

solved) pores (Fig. 3i) and a small amount of intragranular dissolved pores (Fig. 3m). When there are more seepage sand between grains, some residual pores between sand grains (Fig. 3i); when the recrystallization is strong, intercrystalline (dissolved) pores would occur (Fig. 3j).

2.1.2.2. Oolitic dolomite

Oolitic dolomite is also gray and grayish brown, and massive. The ooids account for 60%–85% and are 0.2–0.5 mm in size. The grains, supporting each other, are mostly in point-line contact (Fig. 3k). The ooids can be cemented by dolomite or calcite. Most ooids are concentric ooids, and micrite dolomite in composition. Where the influence of karst is strong, the ooids and freshwater cements are affected by micritization, and have internal fabric of ooids destroyed (Fig. 3l). This type of reservoir rock is characterized by dissolution enlarged

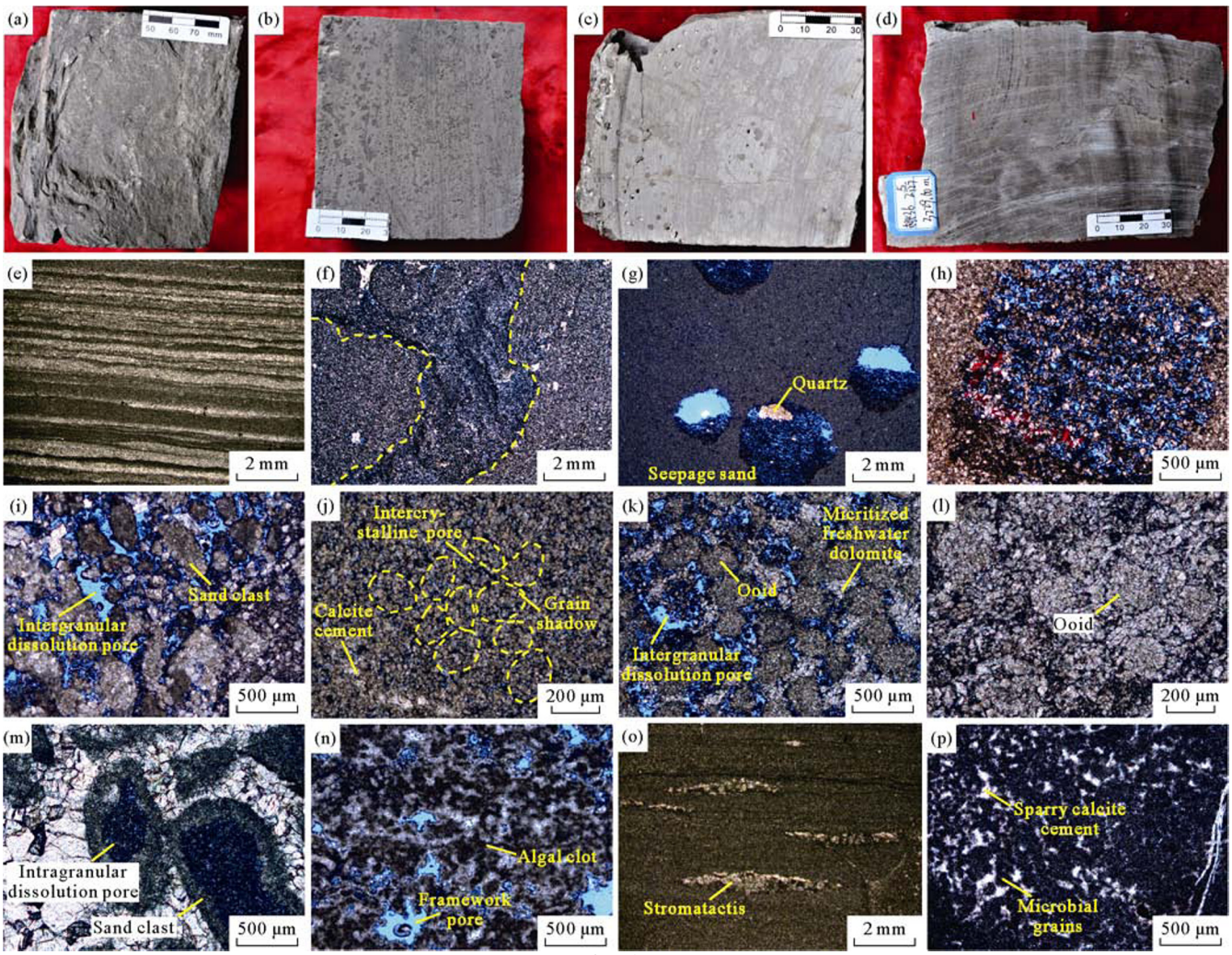

Fig. 3. Petrological characteristics of reservoir rocks in the M_5^4-M_5^1 sub-members of the eastern Sulige gas field. (a) Well S25, core, 3347.95 m, M_5^3 sub-member, gray micrite dolomite, homogeneous mass; (b) Well T51, core, 3429.66 m, M_5^1 sub-member, gray micrite dolomite with moldic pore, the moldic pores are isolated, some of them are enlarged into spongy dissolution; (c) Well SD47-42, core, 3307.87 m, M_5^4 sub-member, brown-gray breccia dolomite, the bedrock is micrite dolomite with moldic pore, and the moldic pores are isolated; (d) Well T36, core, 3229.60 m, M_5^1 sub-member, left: brown-gray stromatolite, the dark layer is dark-gray bacteria-rich micrite dolomite, the bright layer is brown-gray micrite dolomite, right: brown-gray laminated dolomite; (e) Well S25, 3347.95 m, M_5^3 sub-member, lamellar micrite dolomite, the dark layer is argillaceous micrite dolomite, the light layer is powder crystal dolomite, ordinary thin section, single polarized light; (f) Well T6, 3587.78 m, M_5^4 sub-member, micrite dolomite, with intergranular dissolution micropores developed in the bedrock, and karrens partially filled with dolomite breccias and seepage fillings, single-polarized light; (g) Well SD47-42, 3307.87 m, M_5^4 sub-member, micrite dolomite with moldic pore, the moldic pores are partially filled with seepage sand and quartz, single polarized light; (h) Well T2, 3384.86 m, M_5^2 sub-member, micrite dolomite with moldic pore, the moldic pores are isolated, in approximately square shape, and partially filled with calcite, argillaceous seepage sand etc, single polarized light; (i) Well S25, 3355.38 m, M_5^3 sub-member, sparry dolarenite, with intergranular dissolution pores and freshwater dolomite cement, single polarized light; (j) Well T36, 3390.08 m, M_5^4 sub-member, powder crystal dolomite, with grain shadow, intercrystalline (dissolution) pores, and calcite cement, single polarized light; (k) Well T51, 3429.37 m, M_5^1 sub-member, sparry oolitic dolomite, with intergranular pores partially filled with micritized freshwater dolomite cement and seepage silt, single polarized light; (l) Well T51, 3427.54 m, M_5^1 sub-member, micrite oolitic dolomite, with visible residual oolitic structure, intergranular pores partially or completely filled by seepage sand etc, single polarized light; (m) Well Zh97, 3448.44 m, M_5^4 sub-member, sparry dolarenite, with intragranular dissolution pores developed in grains, single polarized light; (n) Well T14, 3615.05 m, M_5^4 sub-member, algal bound clot dolomite, with unfilled framework pores, single polarized light; (o) Well T42, 3407.40 m, M_5^2 sub-member, laminated dolomite, with horizontal laminae and stromatactis fully filled with fine to medium crystalline calcite and other minerals, single polarized light; (P) Well Zh96, 3382.85 m, M_5^1 sub-member, algal bound dolarenite, with calcite cement filling between grains, single polarized light.

residual intergranular pores. Where the influence of karst is strong, micropores between seepage sand may appear (Fig. 3k).

2.1.3. Microbialites

Microbialites are organosedimentary deposits resulted from benthic microbial community trapping and binding detrital sediment and/or sedimentary rock formed in-situ by inorganic or organic induced mineralization related to microbe activities[10]. Microbialites in the M_5^4-M_5^1 sub-members are relatively underdeveloped in the study area. But based on the macroscopic and microfabric characteristics, the common microbialites in the area are divided into clotted dolomite, algal stromatolite, laminated dolomite and algal bound dolarenite. The reservoirs occur mostly in clotted dolomite.

2.1.3.1. Algal bound clotted dolomite

It is brownish gray to gray lamellar dolomite. Microscopically, the microbial clots appear as dark brown-black nets or clusters. It can be seen that they are composed of "peloids" aggregates larger in individual size, with biological framework structure (Fig. 3n). The spaces between the framework are mostly cavities where microorganisms grew, and are usually partially or completely filled with fillings and multi-stage cements, such as seepage sand, medium-coarse crystal dolomite or coarse-giant crystal calcite cement. Meanwhile, framework pores also have the phenomenon of enlargement, marked by their smooth edges. The microbialite reservoir in the area mainly turns up in the clotted dolomite, and has residual framework pores as main storage space.

2.1.3.2. Algal stromatolite and laminated dolomite

Algal stromatolite is composed of cyanobacteria communities that are calcified and micritized, and they have many types of laminae, including near-horizontal, microwave and hemispherical ones (Fig. 3d). Macroscopically, the algal stromatolite has alternate dark bacteria-rich layers and bright bacteria-lean layers. The dark layers are micrite dolomite rich in bacteria, with higher contents of organic matter, thicknesses of 0.2–1.0 mm, and uneven edges. The bright layers are brown gray micrite dolomite with thicknesses from 1 to 5 mm (Fig. 3d).

The laminae edges are often characterized by tiny ups and downs or intermittent distribution, indicating that the existence of irregular microscopic fluctuations on the surface of the microbial mat. Under microscope, framework pores (also known as stromatactis) along bedding are usually seen (Fig. 3o), which are usually explained as the result of wetting and drying of the mound, folding uplift after drying of the bacterial mat, and degassing of decaying organic matter distributed along bedding in the supratidal zone[11]. Laminar dolomite generally appears in the lower part of the microbial mound sequence, and is characterized by the development of nearly horizontal laminae (Fig. 3d) and microscopic stromatactis (Fig. 3o). These two types of dolomites have a high filling degree of geode and poor storage capacity.

2.1.3.3. Algal bound dolarenite

The algal bound dolarenite is formed by cyanobacteria and their secretions bonding and entangling grains. It is gray to dark gray, and usually tight and non-porous, with needle pores occasionally seen on core. Under microscope, accounting for 50%–90%, the sand grains are club, ellipsoid and sphere shape, 0.1–0.7 mm in size, poorly sorted, and well-rounded, with sparry calcite cement filling in between (Fig. 3p). Organic-rich dark micrite envelope can be seen on the edge of the grain, which is caused by cyanobacteria and other microorganisms boring and bonding on the surface of the grain and secreting fine-grained sediments[12]. This kind of rock has grain shape well preserved and weak internal recrystallization. The dissolution is locally inside grain.

2.2. The upward-shallowing sequence

Based on the close observation and description of 353.52 m core from 29 wells encountering the Majiagou Formation in the study area (Fig. 1) and analysis of more than 1,000 thin sections, it is found that high-frequency upward-shallowing sequences are well developed and can be divided into the following four types according to the longitudinal lithologic sequence: (1) argillaceous dolomite (- micrite dolomite) - micrite dolomite with moldic pore (- micrite dolomite) (Fig. 4a, 4b); (2) argillaceous dolomite - algal bound dolarenite - clotted dolomite (Fig. 4c); (3) argillaceous dolomite - lamellar micrite dolomite - grain dolomite-stromatolite - laminated dolomite (Fig. 4d); (4) composite sequence of microbialite, grain dolomite and micrite dolomite with moldic pore (Fig. 4e, 4f).

From the single sequence of micrite dolomite with moldic pore, the lithology changes from argillaceous dolomite (- micrite dolomite) to powder crystal dolomite with moldic pore (- micrite dolomite), reflecting the relatively normal salinity, gradual upward concentration and salinization in initial regressions. Evaporite minerals such as gypsum and halite could precipitate from high-salinity sea water, forming evaporative minerals dispersed in powder crystal dolomite. From the sequence of coexistent microbialite, grain dolomite and powder crystal dolomite with moldic pore, we can see the lithology in upward-shallowing sequence can change from powder crystal dolomite with moldic pore to grain dolomite or microbialite with reverse grading, again to powder crystal dolomite with moldic pore (Fig. 4e, 4f). This indicates that the powder crystal dolomite with moldic pore should be formed in a low energy environment below the wave base. However, in the complex upward-shallowing sequence, the powder crystal dolomite with moldic pore still appears above the microbial mounds and shoals, which may be related to the gradual upward isolation caused by the superimposed migration of the shoals and the synergistic reduction of disturbance depth of the wave base. Based on the morphologic characteristics of the moldic pores, it can be concluded that the paleo-environment should be precipitated from the evaporative seawater, rather than the intertidal-supratidal environment as previously believed.

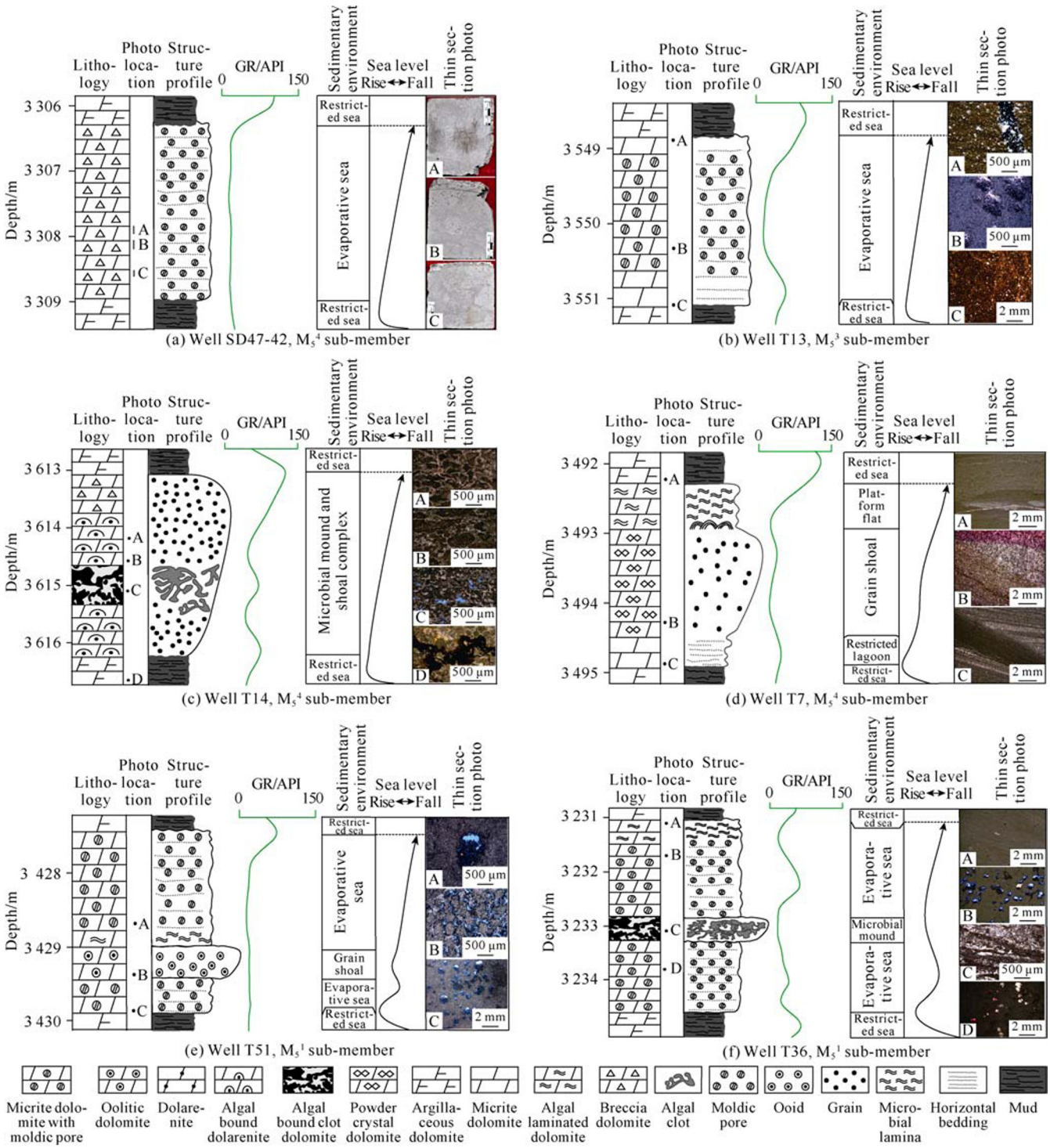

Fig. 4. Types of upward-shallowing sequences in the M_5^4-M_5^1 sub-members in eastern Sulige gas field (GR—natural gamma ray, API).

According to these evidences, there are four kinds of upward-shallowing ancient environment evolution patterns in the M_5^4-M_5^1 sub-members of the study area, namely, restricted sea - evaporative sea, restricted sea - grain shoal - platform flat, restricted sea-microbial mound, and restricted sea-evaporative sea-microbial mound (shoal). Among them, the favorable sedimentary facies such as evaporative sea, grain shoal and microbial mound are mainly in the middle and upper part of the sedimentary sequence. It can be seen from the composite sequence that the upward concentration of palaeoenvironment may also be related to the superimposed migration of microbial mounds (shoals). In the platform, the development of upward-shallowing sequence also indicates that there may be early exposure driven by high-frequency regression.

3. Early exposure of high frequency sequences and karst sequences

Early exposure karst driven by high-frequency sea level fluctuation, also known as penecontemporaneous karst or early epigenetic exposure karst[13], and some scholars also call it eogenetic karst together with exposure karst of sedimentary rocks in the early diagenetic period[14]. In this paper, the early

epigenetic exposure karst driven by high-frequency sea level fluctuation is defined as eogenetic karst.

Previous studies show that eogenetic karst can hardly form ancient weathering crust, but has some typical signatures, like lithologic surface of discontinuity[7], fabric selective dissolution[15], seepage sand and geopetalfabric[16], atmospheric freshwater cements, *in-situ* brecciation[17], dissolution in granophyric or spongy shape[18], dissolution fissures and karrens, small karst caves, and friable halo[19]. Moreover, the eogenetic karst has obvious facies and layer-control features[18].

As mentioned above, the M_5^4-M_5^1 sub-members in the study area are characterized by development of high-frequency upward-shallowing sequences, indicating the area had the paleo-geographic background of eogenetic karst. Based on macro and micro observation of a large number of cores, we found that they have the following karst and sequence characteristics.

3.1. Signatures of high-frequency eogenetic karst

(1) Lithologic surface of discontinuity and exposure surface. The top of one high-frequency sedimentary cycle and the overlying initial transgression deposit of another cycle are often separated by a interface of lithologic abrupt change. This interface mainly appears as abrupt change from dark to gray mudstone to micrite dolomite (or mold-bearing dolomite) or from dolomitic mudstone to amorphous *in-suit* breccia (Fig. 5). Typical sequences on cores from Wells T42 and T14 show that the lamellar dark dolomitic mudstone or argillaceous dolomite above the abrupt lithologic change interface gradually transforms upward to lamellar dolomite or micrite dolomite, indicating that it should be the overlying sedimentary product rather than the filling of the karst system in Caledonian - early Hercynian period (Fig. 5). Due to the slope break of the underlying karst micro-landform, the sediment of initial high-frequency transgression cycle above the exposure surface often has gravity faults and collapse deposit (Fig. 5i). In the karst system of the early cycle, typical late high-frequency transgressive sediment filling characteristics can be seen (Fig. 5h, 5j), which are the most direct evidence of high-frequency eogenetic karst.

(2) Fabric selective dissolution and seepage silt fillings

The selective dissolution occurs mostly in micrite dolomite with moldic pore (Fig. 3c), which is characterized by the formation of moldic pores. Selective dissolution of grain dolomite is occasionally seen and mainly appears as intragranular selective dissolution pores (Fig. 3m). Most of the moldic pores are partially filled with calcite and dolomitic seepage sand (Fig. 3g), and a few moldic pores are filled with loose seepage sand in the middle and lower part, and without filling or filled with calcite in the upper part, constituting the geopetal structure (Fig. 3g).

(3) Spongy dissolution and brecciation

Spongy dissolution is a typical feature of eogenetic karst[18]. This dissolution characteristic is commonly seen in the high-frequency cycles of the M_5^4-M_5^1 sub-members. The rocks suffering spongy dissolution include original dark micrite dolomite and brownish gray micrite dolomite, distinct in color, they appear as dark and light patches (Fig. 3b). Brecciation generally occurs in the high-frequency cycles of M_5^4-M_5^1 sub-members, and even in some whole cycles. The breccias are light in color and vary widely in size, and most of them are amorphous or plastic. Some breccias can piece together with adjacent surrounding rocks or breccias (Fig. 5h, 5j), and seepage silt fillings or later high-frequency transgression sediments may fill in between the breccias (Fig. 5h, 5j, 5l, 5m).

(4) Dissolution fissures, karrens, small karst caves and fillings

The dissolution fissures, karrens and small karst caves are abundant in the high-frequency cycles of the M_5^4-M_5^1 sub-members. According to their occurrence characteristics, they can be divided into vertical dissolution karrens, horizontal fissures and horizontal karst caves. The phenomenon of dissolution fissures and karrens cutting moldic pores jointly can be seen. Most of the dissolution fissures and karrens turn up in the upper part of the cycle, while the horizontal dissolution fissures and layered karst caves occur in the middle and lower part of the cycle. But the middle and upper part can also have horizontal dissolution fissures and small caves (Fig. 6). These karst systems have irregular boundaries and various fillings such as seepage sand, *in-situ* breccia and later initial transgression cycle sediments (Fig. 5j, 5k). Some small caves are filled with mud and calcite, forming geopetal structure (Fig. 5l).

(5) Dedolomitization and freshwater cements

Affected by exposure karst, the middle and upper part of the high-frequency upward-shallowing sequence is often dedolomitized, thus forming the limy breccia (Fig. 5d, 5e, 5g, 5h) and the limy dolomite with spongy dissolution (Fig. 5k, 5l). At the same time, in the grain dolomite, clean dolomite cement particles can be seen on one side of the grains or at the contact point of the grains (Fig. 3k), and some of them are micritized due to the influence of continuous freshwater (Fig. 3l). This kind of freshwater dolomite is a typical signature of early atmospheric freshwater seepage zone[20–21].

According to the characteristics of the overlying high-frequency transgression sediments entering the early karst system, it is confirmed that there are obvious high-frequency sea-level-driven exposures and eogenetic karst in the M_5^4-M_5^1 sub-members, accompanied by spongy dissolution, *in-situ* brecciation and atmospheric freshwater cements, which are sufficient to prove that the carbonate rocks of the M_5^4-M_5^1 sub-members have suffered superimposed eogenetic karst. It can be inferred from the general brecciation in the upper part of the high-frequency cycle in the region that the mid-to-long term exposure happened during the penecontemporaneous period[22].

As mentioned above, the original rock of micrite dolomite with moldic pore may be micrite dolomite containing evaporative minerals, because the solubility of gypsum and halite is 30 to 70 times that of carbonate sediments[23–24], when the exposure is long and at high frequency, the evaporative minerals would first dissolve and migrate to form moldic pores. Therefore, it is safe to say that the high-frequency eogenetic karst is the

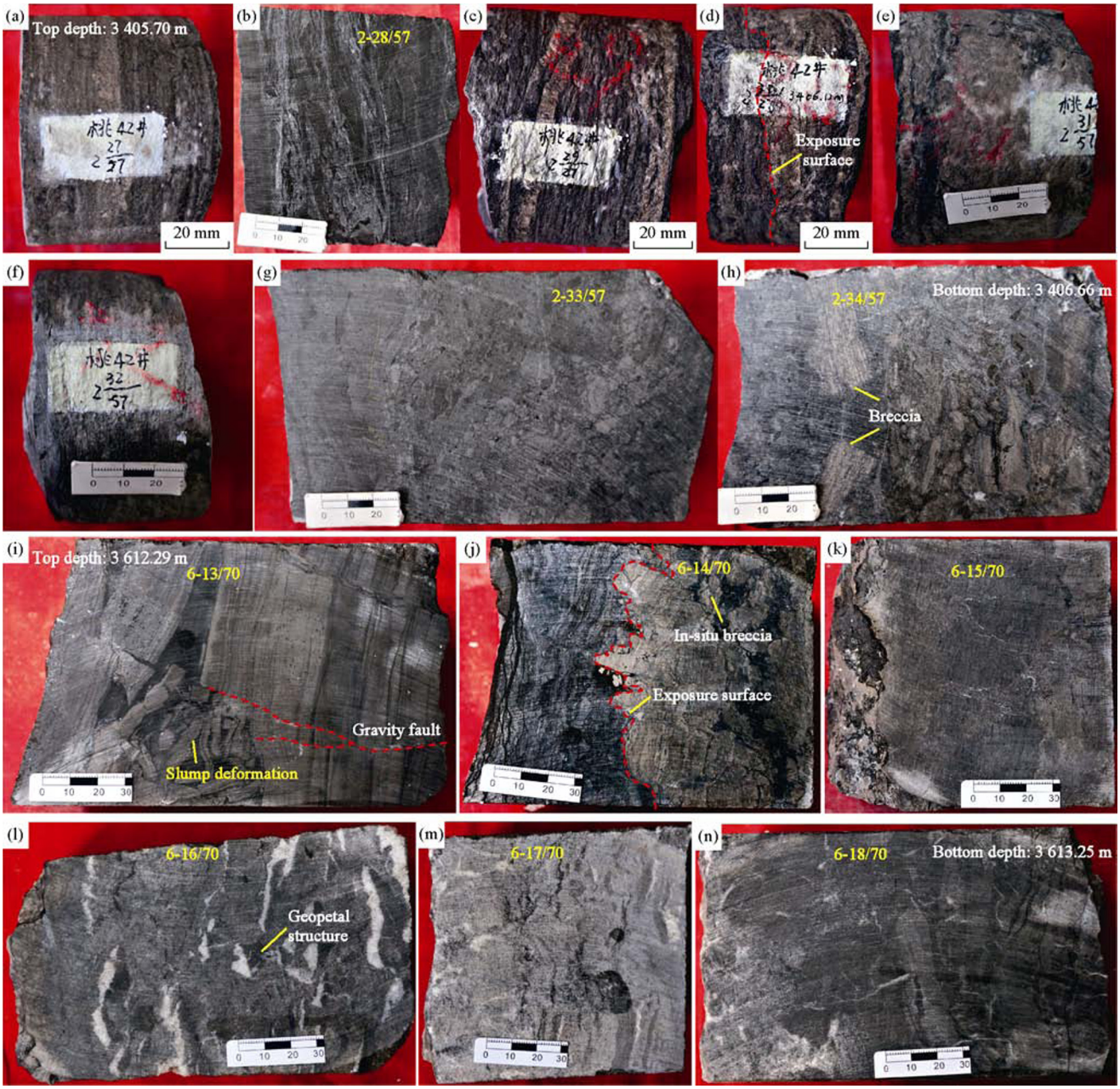

Fig. 5. Eogenetic karst features in the M_5^4-M_5^1 sub-members of eastern Sulige gas field. (a) Well T42, core, 3 405.78 m, M_5^2 sub-member, brownish gray micrite dolomite, the lower part is black argillaceous dolomite; (b) Well T42, core, 3 405.90 m, M_5^2 sub-member, dark gray argillaceous dolomite with black transgression argillaceous sediments; (c) Well T42, core, 3 406.02 m, M_5^2 sub-member, black argillaceous dolomite, with thin layers of brownish gray micrite dolomite; (d) Well T42, core, 3 406.12 m, M_5^2 sub-member, exposure surface, with black argillaceous dolomite above and brownish gray limy breccia dolomite with dedolomitization below; (e) Well T42, core, 3 406.22 m, M_5^2 sub-member, brown gray gray-breccia dolomite, dedolomitization; (f) Well T42, core, 3 406.28 m, M_5^2 sub-member, brown gray limy micrite dolomite, dedolomitization; (g) Well T42, core, 3 406.48 m, M_5^2 sub-member, brownish gray to gray-breccia dolomite, dedolomitization; (h) Well T42, core, 3406.66 m, M_5^2 sub-member, brownish gray to gray breccia dolomite, de-dolomitized; (i) Well T14, core, 3612.48 m, M_5^4 sub-member, brownish gray algal stromatolite, with gravity fault and collapse deformation; (j) Well T14, core, 3 612.66 m, M_5^4 sub-member, exposure surface, with grayish black argillaceous dolomite above and de-dolomitized brownish gray limy breccia below, and high-frequency overlying transgression sediments filling between breccias; (k) Well T14, core, 3612.80 m, M_5^4 sub-member, brownish gray limy dolomite with spongy dissolution; (l) Well T14, core, 3 612.96 m, M_5^4 sub-member, dark gray limy dolomite with spongy dissolution, dedolomitization, horizontal karst caves fully filled with seepage fillings and calcite; (m) Well T14, core, 3 613.06 m, M_5^4 sub-member, de-dolomitized light gray limy dolomite, dedolomitization; (n) Well T14, core, 3 613.25 m, M_5^4 sub-member, de-dolomitized gray limy dolomite, dedolomitization.

main force driving the formation of moldic pores in the M_5^4-M_5^1 sub-members.

3.2. High-frequency eogenetic karst sequences

Although the eogenetic karst driven by high-frequency exposure can be confirmed by cores and microscopic petrological evidence already, in order to provide more intuitive petrological evidence, the following three complete core sequences are selected and analyzed with the microscopic characteristics of typical sequences.

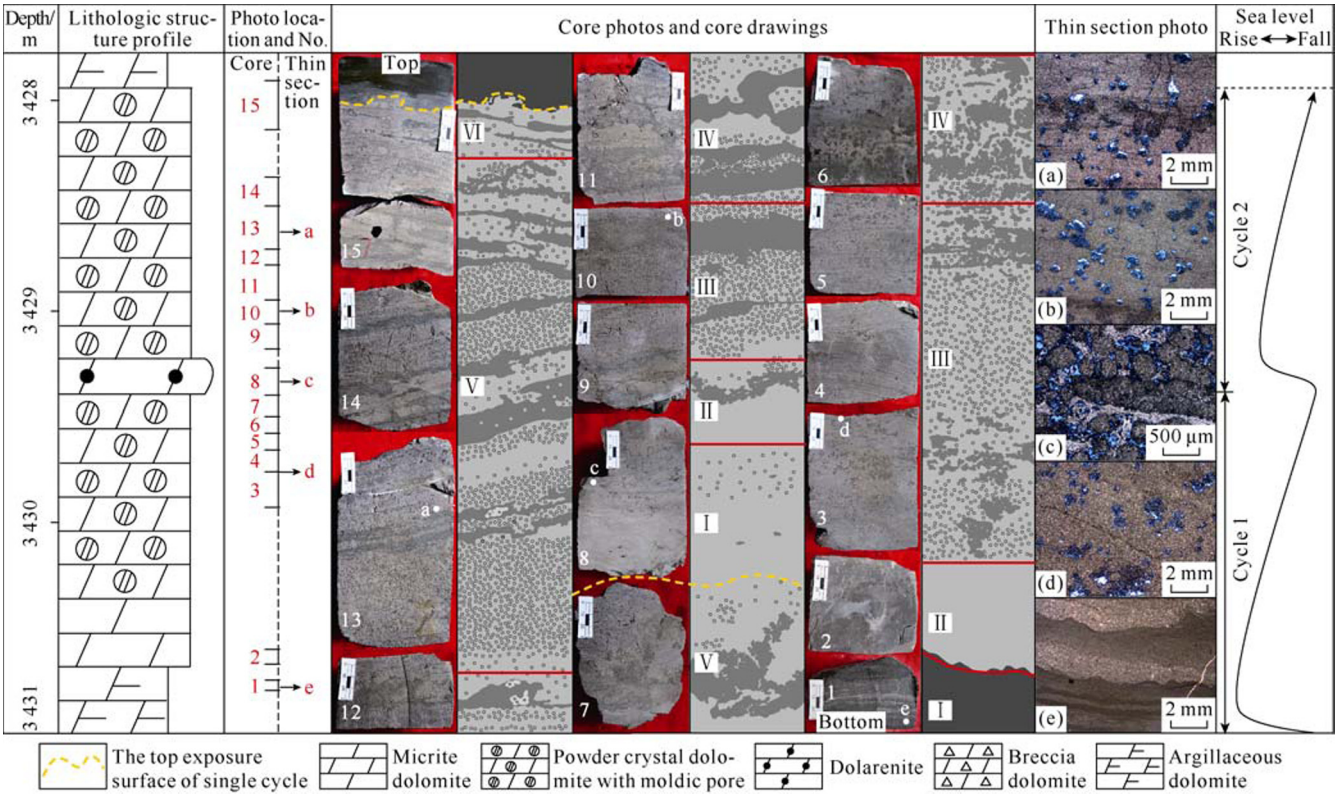

Fig. 6. Upward-shallowing sequence and karst characteristics of section 3427.72–3430.83 m in Well T51. (a) Micrite dolomite with moldic pore, connected dissolved moldic pores are highly filled, cast thin section, single polarized light; (b) micrite dolomite with moldic pore, connected dissolved moldic pores are highly filled, cast thin section, single polarized light; (c) sparry grain dolomite, containing leaf-like gravel grain and freshwater dolomite cements, cast thin section, single polarized light; (d) micrite dolomite with moldic pore, cast thin section, single polarized light; (e) argillaceous micrite dolomite interbedded with micrite dolomite, ordinary thin section, single polarized light.

3.2.1. Cycle 1: lamellar argillaceous dolomite - micrite dolomite - micrite dolomite with moldic pore

The top and bottom of the cycle are separated from the high-frequency cycle by unsmooth interface of abrupt lithologic change. According to the lithologic association and karst characteristics, the cycle can be divided into the following 5 units from bottom to top (Fig. 6):

(1) Unit I (17 cm thick): gray lamellar micrite dolomite, which represents the rapid transgression deposit in the early stage of the cycle.

(2) Unit II (28 cm thick): tight gray argillaceous micrite dolomite, which is a water-barrier layer of exposure karst with little karst signs.

(3) Unit III (78 cm thick): brownish gray micrite dolomite with moldic pore, in which the karst sign is the moldic pore formed by dissolution and migration of evaporative minerals. At the same time, initial small-scale spongy dissolution due to selective dissolution and seepage fillings occurs in local parts.

(4) Unit IV (13 cm thick): brownish gray micrite and micrite dolomite with moldic pore, with obvious spongy dissolution, and brecciation in local parts due to the cutting of dominant karst channels.

(5) Unit V (15 cm): brownish gray micrite dolomite with moldic pore. Brecciation occurs due to the cutting of dominant karst channels formed by gradual connection of moldic pores and filling of seepage silt fillings, the remaining moldic pores have poorer storage capacity due to filling of seepage silts.

Based on sequence characteristics, the vertical karst sequence can be divided into near-surface zone (near-surface breccia zone, unit V) - vertical vadose zone (spongy dissolution, units III and IV). In terms of scale, this sequence is characterized by well-developed vertical vadose zone. Compared with the classical weathering crust karst zoning, it lacks deep slow-flow zone and is smaller in karst zone. At the same time, the horizontal phreatic zone of this cycle has just begun to develop, indicating that the karst strength is moderately weak, but has significant enhancement to the reservoir quality.

3.2.2. Cycle 2: grain dolomite - micrite dolomite with moldic pore

The top and bottom of the cycle are all uneven abrupt lithologic change interfaces. The bottom is the boundary between the thin-layered micrite dolomite and the underlying brecciated micrite dolomite. The top is the boundary between dark gray argillaceous micrite dolomite and micrite dolomite. The cycle can be divided into 6 units from bottom to top (Fig. 6):

(1) Unit I (15 cm thick): brownish gray dolarenite, which represents rapid transgression and enhanced hydrodynamics in the sea area; the karstification of this unit is relatively weak and appears in the forms of dissolution enlargement of intergranular pore and seepage sand filling.

(2) Unit II (10 cm thick): brownish gray dolarenite, which forms a reverse grading sequence with Unit I. A network of

nearly horizontal dominant karst channels occurs at the bottom of this unit, which cuts and causes brecciation of the original rock to some extent.

(3) Unit III (10 cm thick): brownish gray micrite dolomite with moldic pore, which shows weak karstification in the form of spongy dissolution.

(4) Unit IV (23 cm thick): brownish gray micrite dolomite with moldic pore, which is characterized by the development of near-horizontal dominant karst channels and centimeter-sized near-horizontal karst caves. But the fillings are seepage silts and pseudo-breccias formed by the cutting of dominant karst channels, with no mechanical breccias, indicating that the karst caves in the horizontal phreatic zone are in the initial development stage. This unit has poorer physical properties due to mixed filling.

(5) Unit V (68 cm thick): brownish gray micrite dolomite with moldic pore, which is characterized by development of moldic pores and near-horizontal dissolution fissures. The fillings of the dissolution fissures is similar in color with the sediment of the initial transgression in the next cycle, and is composed of seepage sand and argillaceous material on the microscopic level. On the core, in the lower part of the horizontal dissolution fissures is micrite dolomite with fewer moldic pores, representing the salinity decrease of sea water. The development of the horizontal dissolution fissures may be related to the intermittent replenishment of seawater and the drop of salinity. Also, the micrite dolomite without moldic pore could act as a water-blocking layer, leading to the development of horizontal dissolution fissures above it.

(6) Unit VI (4 cm thick): brownish gray micrite dolomite with moldic pore, with near horizontal dissolution fissures in the lower part and brecciation in the upper part. The fillings of the karst system has some initial transgression sediments of the next cycle mixed in obviously, which also proves from the sequence characteristics that the karst with such characteristics is the eogenetic karst driven by high-frequency exposure.

According to the karst characteristics, the cycle 2 can be divided into near-surface zone (with weak brecciation and nearly horizontal dissolution, unit VI) - vertical vadose zone (with selective dissolution and nearly horizontal dissolution, unit V) - horizontal phreatic zone (with small horizontal cave and in-situ breccia, unit IV) - deep slow-flow zone (with spongy dissolution, units I-III). Compared with cycle 1, the karst zoning tends to be obvious, and is still characterized by the development of vadose zone karst. The difference from cycle 1 is that near-horizontal dissolution occurs in the vadose zone due to the difference in lithology. In terms of scale, it has more developed horizontal phreatic zone than cycle 1, but has no transport breccia or cave collapse breccia, which indicates that the karst intensity is still moderate but stronger than the cycle 1. In general, the karst still plays a constructive role in reservoir reformation.

3.2.3. Cycle 3: breccias

This kind of cycle is characterized by karst breccia in the whole upward-shallowing sequence, which forms a stratified breccia section. The breccias vary in color and lithology, including gray micrite dolomite, brownish gray micrite dolomite, micrite dolomite with moldic pore, and grain dolomite, etc., but all breccias are still from same source (Fig. 7). The fillings between breccias are dolomite sand, small breccia, seepage silt, calcite formed by cave chemical deposition, and overlying argillaceous or micrite sediments of the high-frequency transgression (Figs. 5h, 5j and 7). The breccias are mixed in size and shapes (ones with sharp edges and rounded ones), reflecting the causes of mechanical transportation and collapse. This sequence indicates that it is strongly influenced by karstification and has a certain scale of horizontal karst caves and shallow subsurface river system formed. Later, due to the underground river carrying breccias and the overall collapse of the cave, the cycle shows overall brecciation, which may be caused by long exposure time and high karst intensity, or it might be controlled by the karst geomorphic unit as it was in the lower slope of local uplands during high-frequency exposure. According to statistics of a large number of overall brecciation sequences, with the space between breccias prone to be filled with dolomite sand and overlying high-frequency transgression stage sediments, the karst breccia could basically lose storage capacity (Fig. 7).

4. Facies-controlled eogenetic karst process and its control on reservoirs

4.1. Genesis of fabrics in the eogenetic karst

The eogenetic karst is distinguished from the weathering crust karst in the late diagenetic stage by the spongy dissolution, *in-situ* brecciation and seepage silt fillings[16–17]. The upper part of the high-frequency cycle in the M_5^4-M_5^1 sub-members of the Majiagou Formation is usually characterized by brecciation. As atmospheric freshwater flew along the fissures between dolomite crystals developed in the early stage, moldic pores represented by gypsum and salt moldic pores would be formed by dissolution of evaporative minerals easy to migrate first (Fig. 3c). Then with the establishment of the fluid seepage system composed of intergranular dissolution pores and moldic pores, when the karstification went on further, the adjacent moldic pores and intergranular dissolution micropores would gradually join to form a dominant karst channel or an area strongly affected by karstification (Fig. 6). If the karst influence time in the dominant channel was short, the channel would be characterized by dissolution of *in-situ* materials or grain size reduction. In the dominant channels, due to the different lithological components, the rocks appear in patch pattern, so the dissolution is named patchy dissolution (or spongy dissolution). And the boundary between the dominant karst channel and the original rock is relatively fuzzy (Fig. 3b). When the karstification went on further, the dominant channels would gradually connect to form a network system, cutting the rocks to form *in-situ* breccias (Fig. 3c). The breccia morphology is controlled by the three-dimensional morphology of the dominant channel, thus showing amorphous or plastic characteristics, and some adjacent breccias

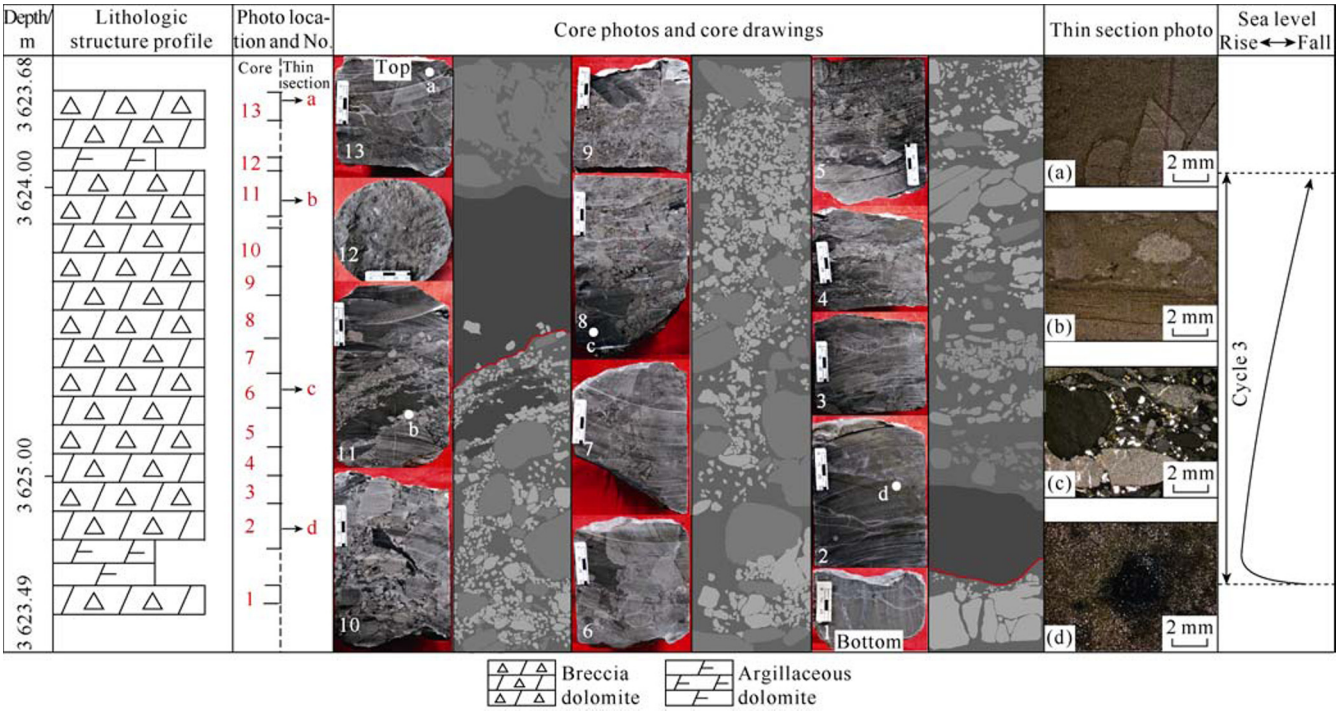

Fig. 7. Upward-shallowing sequence and overall brecciation of section 3623.68–3625.49 m in Well T44. (a) Breccia dolomite, micrite dolomite filling between breccias, ordinary thin slice, single polarized light; (b) breccia dolomite, micrite dolomite filling between breccias, ordinary thin slice, single polarized light; (c) breccia dolomite, the breccias are light gray and dark gray, the space between breccias is filled with mud and quartz etc, ordinary thin slice, single polarized light; (d) micrite dolomite, rich in mud, ordinary thin slice, single polarized light.

can be pieced together (Fig. 5h, 5j). When karstification went on further, the dissolution products in the dominant channels would be move away gradually to form caves due to chemical dissolution and mechanical transportation, but such caves are mainly filled with *in-situ* breccias, seepage sand and overlying high-frequency transgression stage sediments (Fig. 5j).

4.2. Karst dynamic evolution stage

As mentioned above, multiple upward-shallowing sequences superposed vertically can be identified on the core, suggesting frequent sea-level fluctuations and high-frequency sedimentary cycles. For a single upward-shallowing cycle, different sedimentary cycles have different degrees of karst development, such as selective dissolution and overall brecciation. Generally, karst development gradually weakens from top to bottom, and the middle and lower parts of a cycle usually have dissolution pores, spongy dissolution, and a small amount of breccia, while the top part of a cycle is usually characterized by the development of karrens and a large amount of breccia (Figs. 6 and 7). Therefore, it is inferred that the degree of karst development is controlled by the exposure time of the top of a single sedimentary cycle or the eogenetic karst micro-topography unit, and the longer the exposure time or at the edge of the highlands, the greater the karstification intensity is. According to the above karst development characteristics, the three stages of karst development and evolution can be roughly divided (Fig. 8):

4.2.1. Selective dissolution and migration of soluble minerals

In the early stage of diagenesis, in the symbiosis system of evaporative minerals and carbonate sediments (Fig. 8a), the sediments that had just or were still undergoing seawater diagenesis were exposed for a short period, and the original seawater fluid in the pores was replaced by atmospheric freshwater. At this time, different components and fabrics in the sediments are different in stability, among which evaporative minerals such as gypsum and halite have much higher solubility than carbonate sediments[23–24], thus soluble minerals such as gypsum and halite would be dissolved first to form moldic pores (Fig. 8b), leading to the so-called selective dissolution. At this time, the intercrystalline dissolution micropores in the matrix dolomites have not developed in large quantity, and the reservoir spaces dominated by moldic pores were relatively isolated. The reformation of the reservoir was reflected in the improvement of porosity, but the permeability was not improved much (Fig. 8b).

4.2.2. Formation stage of karst zoning

With the increase of exposure time or the karst intensity, the karst water transport system made up of the early pore systems, such as intergranular dissolution micro-pores and moldic pores, was improved, and the dominant karst channels began to develop in large quantities. At the top of the cycle, the developed network channel system also led to *in-situ* brecciation as the dissolution made grains shrink and micritized, while the dominant channels turned poor in physical properties due to the mixed filling of seepage fillings or initial overlying transgression stage sediments. Affected by the atmospheric freshwater, the middle-upper part of the cycle had brecciation or spongy dissolution under the cutting of karst channels. If the

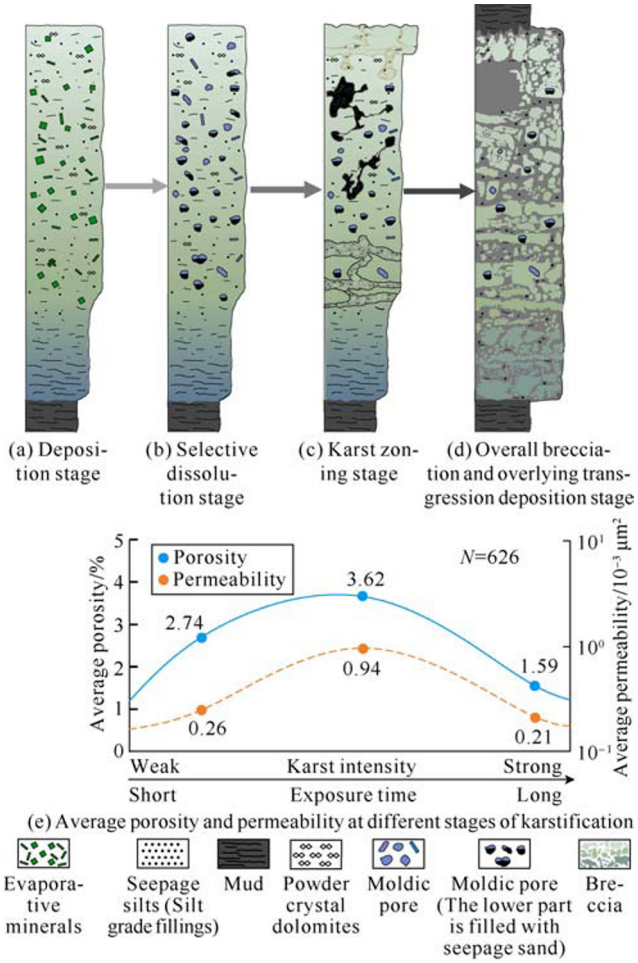

Fig. 8. Evolution stage and physical characteristics of karst development.

original rock was grain dolomite, there might be typical freshwater dolomite cements developed (Fig. 3k). At the lower part of the cycle, the low-permeability layer formed by high-frequency transgression acted as a water-proof layer, making the karst water mainly flow slowly horizontally and gradually giving rise to pseudo-breccias cut by the dominant channels (Fig. 8c). If karst development terminated due to overlying high-frequency marine transgression sediment, the karst dominant channel system would be filled with seepage sand, *in-situ* breccias or overlying high-frequency transgression sediments (Fig. 5h, 5j). At this stage, on the one hand, the physical properties of the karst channels became poorer due to filling, but due to the difference of fabrics caused by karst and the influence of static pressure of the overlying ground, fractures were likely to occur. On the other hand, due to the further development of intergranular dissolution in the matrix, a composite reservoir composed of intergranular dissolution pores and moldic pore were formed, with reservoir property further improved (Fig. 8c).

4.2.3. Stage of excessive karst (overall brecciation)

When the exposure time was long or the intensity of karst was greater, dominant karst channels in the upper and middle part of the cycle continued to expand, and the brecciation characteristics became more obvious, and the reservoir with early moldic pores was destroyed (Fig. 3c). The horizontal phreatic zone in the middle and lower part could have layered karst caves due to dissolution and mechanical transportation, but as the rock in early diagenesis was low in consolidation, the karst cave were likely to be filled with discrete breccias, sand and seepage silts. Or the whole section of the sedimentary sequence might collapse due to static pressure loading of overlying sediments, resulting in brecciation of the whole section, thus forming a chaotic breccia section with different breccias and fillings (Fig. 7). At this time, the physical properties of the karst channels became worse due to the filling of fine particles (Fig. 8d).

4.3. Effects of eogenetic karst on reservoir physical property

During the dissolution process, eogenetic karst is obviously controlled by lithology and litho-facies, and has distinct "facies-controlled" characteristic[18]. The reservoir rocks in the M_5^4-M_5^1 sub-members of the Majiagou Formation in the study area include micrite dolomite with moldic pore, grain dolomite and microbialite, which is characterized by well-developed moldic pore, intergranular (dissolved) pore and (dissolved) residual framework pore respectively. These rocks with good porosity and permeability are obviously reformed by karstification and characterized by spongy dissolution, karrens, karst caves, brecciation and mixed fillings (Fig. 3b, 3c). However, the mold-bearing dolomite is usually dense and less subject to karst reformation (Fig. 3a, 3e). In a word, the carbonate reservoirs of the M_5^4-M_5^1 sub-members Formation in the study area is the genesis of facies-controlled eogenetic karst, and the reservoir prediction should be regressed to the sedimentary micro-facies and the reservoir development rules in the early diagenesis stage.

According to the intensity of karst, the evolution stage of karst can be divided into the stage of selective dissolution and migration of soluble minerals, the stage of karst zoning and the stage of excessive karst. In this study, 626 groups of samples affected by karst were classified according to the above three stages by combining the physical properties of the reservoir with the evolution stage, and then the relationship between the karst stage and the reservoir was discussed. The results show that the soluble minerals formed in the deposition stage, such as gypsum and halite, were more likely to be selectively dissolved, resulting in the formation of isolated moldic pores, with an average porosity of 2.74% and an average permeability of 0.26×10^{-3} μm^2 (Fig. 8b, 8e). Subsequently, because of the dissolution enlargement of moldic pores, formation of intercrystalline dissolution pores in the matrix and the differences in rock fabrics, fractures were likely to come up, connecting isolated dissolution pores, and greatly improving the permeability of the reservoir. At this point, the reservoir spaces included dissolution pore, intergranular pore and intergranular dissolution pore; also, the reservoir physical properties were the best, with an average porosity of 3.62%

and an average permeability of 0.94×10^{-3} μm^2 (Fig. 8c, 8e). With the increase of dissolution intensity, brecciation and sand filling between breccias occurred, the main pore types were residual moldic pore and residual matrix micropore. At this time, the average porosity was the lowest, only 1.59%, and the permeability was also very low, 0.21×10^{-3} μm^2 (Fig. 8d, 8e).

Therefore, it is reasonable to believe that with the increase of exposure time, the karst strength would change from weak to strong, and the karst influence area expand from non-development to the whole upward-shallowing cycle, and the rock gradually turn from well preserved to overall brecciation. Meanwhile, the porosity and permeability would get better first and then get worse, indicating that when the exposure or karstification intensity in the early to middle stage is weak to moderate, the eogenetic karst would improve the reservoir quality, but when the karstification intensity increases further, the reservoir would be damaged.

4.4. Petroleum geologic significance of Caledonian - early Hercynian weathering crust karst

4.4.1. Limited reformation to reservoirs

As mentioned above, the three types of reservoir rocks in the M_5^4-M_5^1 sub-members in the study area are all related to the facies-controlled high-frequency eogenetic karst in genesis. Meanwhile, how much the contribution of Caledonian - early Hercynian weathering crust karst to reservoir formation is, whether karst geomorphic units control reservoir development become the focus of the problem. For this reason, the core intervals above and below the weathering crust in Well Sh243 and the reservoir profiles through different karst geomorphic units are selected as examples for illustration in this study.

The core interval at the top of Ordovician in Well Sh243 shows direct contact between the dolomite of the M_5^1 sub-member and overlying bauxitic mudstone of the Benxi Formation. Its weathering crust karst has the following characteristics (Fig. 9): (1) Karst influence depth is small, generally several meters to ten meters. (2) The karst system is filled with bauxitic mudstone of the overlying Benxi Formation, and the karst reformed section shows variegation with the oxidation characteristics and is mixed with some coarse-grained terrigenous clasts. (3) The karst zone also basically overlaps with the early porous layers, and reformed them into a massive rock of variegation, for example, the 3227.05–3227.45 m well interval. (4) In the vicinity of the weathering crust, small residual caves are formed by karst. These features can be distinguished from the typical features of high-frequency eogenetic karst, such as moldic pore, spongy dissolution and *in-situ* brecciation. In general, Caledonian-early Hercynian weathering crust karst superimposedly reformed and destructed the early porous layers, but also gave rise to a small number of small caves in the early porous layers. This characteristic is consistent with the rare drilling break and leakage in more than 1500 wells drilled in the study area, and also indicates that there are significant differences between the characteristics of large fissures and caves in the dolomite weathering crust karst and limestone weathering crust karst.

To further illustrate the control of dolomite weathering crust karst on reservoir development, based on the existing logging interpretation results, drilling profiles through different geomorphic units (karst highlands, karst slopes and karst

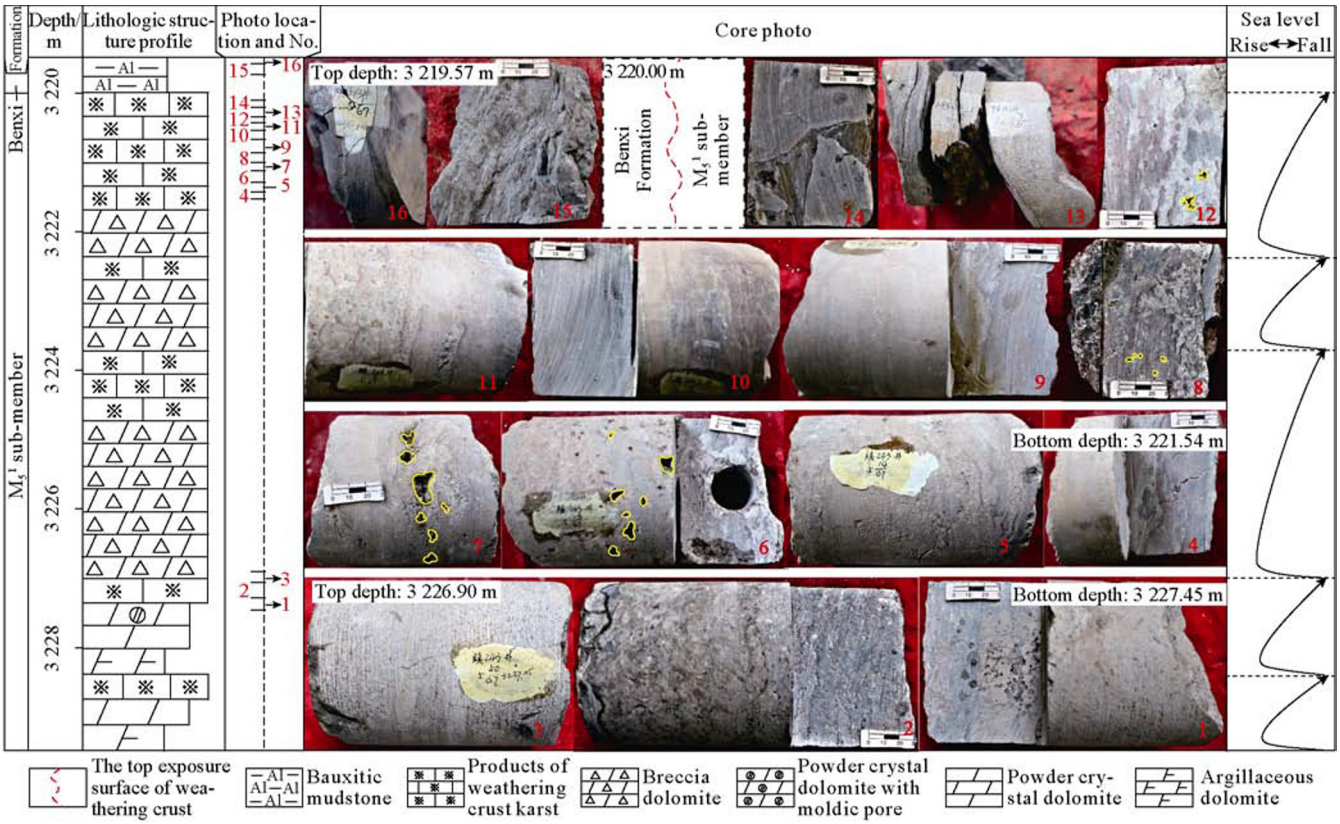

Fig. 9. Karst and reservoir characteristics of the cored section 3219.57–3229.57 m in Well Sh243.

grooves) were selected to compare the reservoir features. It is found that the development of the reservoir controlled by lithofacies is related to the preservation of strata, while has little relationship with karst geomorphologic units. When different geomorphic units all have M_5^4 sub-member strata remained, lithofacies-controlled reservoirs occur in the upper and middle part of the sub-member in each well. However, when karst highlands and slopes all have M_5^3 sub-member strata remained, the development of reservoir may be controlled by lateral variation of lithofacies. For example, the M_5^3 sub-member reservoirs in wells T13 and T39 have similar development positions. In this case, part of the reservoir section is missing due to erosion of karst groove, so the development of such facies-controlled reservoirs is easily mistaken to be related to karst paleogeomorphology (Fig. 10).

4.4.2. Weathering crust karst controls hydrocarbon accumulation by connecting source and reservoir with erosion grooves

Compared with the Ordovician Lianglitage Formation, Yingshan Formation in Tarim Basin and the Middle Permian Maokou Formation in Sichuan Basin, the M_5^4-M_5^1 sub-members in the study area are a polycyclic formation with dispersed and mixed dolomite and evaporative minerals. Under the influence of facies-controlled eogenetic karst, stratified reservoirs stable in stratigraphic horizon with lateral uneven changes often occur in study area (Fig. 11a). During the Caledonian and early Hercynian periods, the study area was subjected to long-term atmospheric freshwater leaching and weathering, and thus a unique weathering crust karst paleogeomorphology with grooves in China turned up, destructing the continuity of the early stage quasi-stratified reservoirs controlled by lithofacies (Fig. 11b)[25].

On the other hand, after Caledonian-early Hercynian karst, the weathering crust was covered by upper Paleozoic coal measures. The study shows that the weathering crust gas pools in the middle and eastern Ordos Basin have two major gas sources: oil-type gas produced by the marine argillaceous carbonate source rock with low abundance in Majiagou Formation[26]; and the coal-derived gas generated by coal measure source rock of the upper Paleozoic and a small amount of oil-type gas generated by Carboniferous limestone[27–28]. The natural gas components in the study area are dominated by coal-derived gas and supplemented by oil-type gas, indicating that the major source rock in the study area is the upper Paleozoic coal-measure source rock overlying the weathering crust[29]. Therefore, the most important role of karst and erosion in the Caledonian-early Hercynian period is to make the

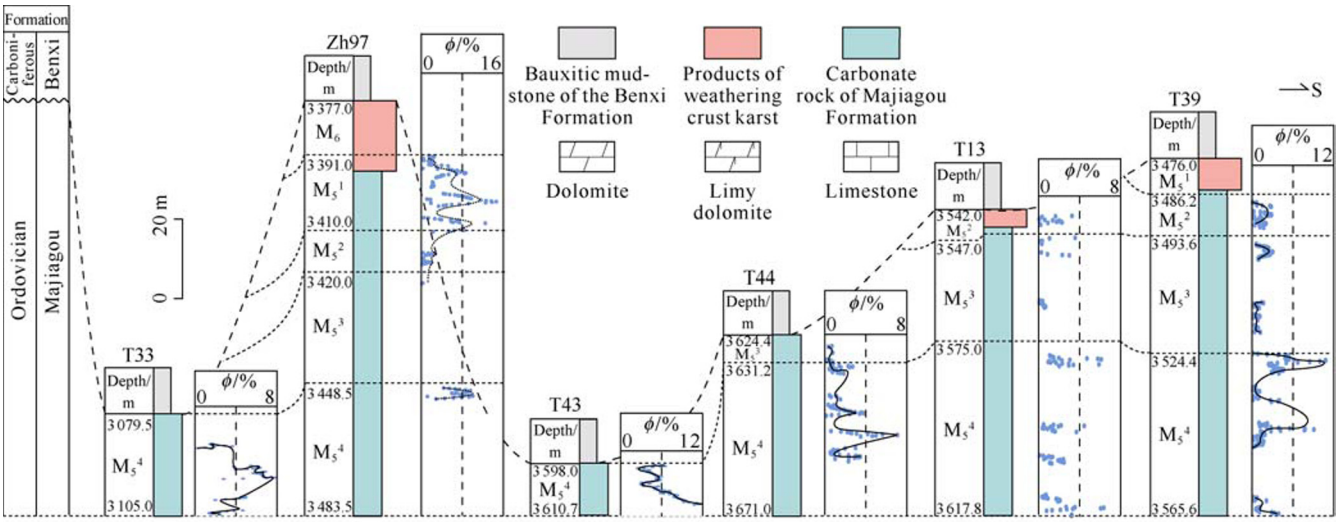

Fig. 10. Comparison of reservoir profiles across different karst geomorphic units (leveled bottom of the M_5^4 sub-member, ϕ—porosity,%, profile position see in Fig. 1).).

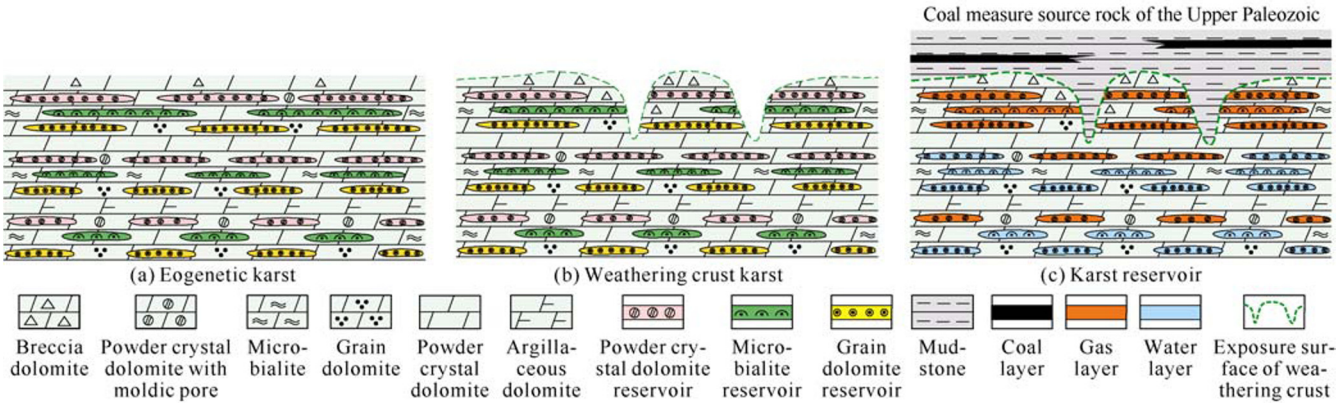

Fig. 11. Schematic diagram of "facies-controlled eogenetic karst controlling reservoirs and weathering crust karst in Caledonian - early Hercynian period controlling hydrocarbon accumulation" in eastern Sulige gas field.

lower Paleozoic reservoir embed with the upper Paleozoic coal-measure source rock, forming the side-by-side source rock and reservoir and source rock below reservoir configurations, allowing the lateral and vertical close migration and accumulation (Fig. 11c).

In general, the weathering crust karst in Caledonian - early Hercynian period destroyed the pores formed by the eogenetic karst, and only produced a small number of dissolution pores in the upper part of the cycle, showing that the Caledonian - early Hercynian karst has limited improvement to the reservoir, even has mainly destruction to reservoir, and the reservoir is still controlled by the eogenetic karst. But from the perspective of formation filling characteristics in the later period, the more important thing is that the grooves formed by weathering crust karst in Caledonian - early Hercynian period makes the source rock contact with the reservoir directly, thus controlling the hydrocarbon accumulation. All in all, it is concluded that the M_5^4-M_5^1 sub-members has the petroleum geological characteristics of facies-controlled eogenetic karst controlling the reservoir and the weathering crust karst in Caledonian - early Hercynian period controlling hydrocarbon accumulation. According to this model, the groove system with favorable conditions for reservoir formation will be the favorable area for further exploration.

5. Conclusions

The reservoir rocks in the M_5^4-M_5^1 sub-members in eastern Sulige gas field mainly include powder crystal dolomite with moldic pore, grain dolomite and microbialite. These lithologies vertically combine into four kinds of high-frequency upward- shallowing sequences: restricted sea - evaporative sea, restricted sea - grain shoal - platform flat, restricted sea - microbial mound, and restricted sea - evaporative sea - microbial mound (shoal).

Typical characteristics of high frequency exposure in early diagenesis include abrupt lithologic change interface, selective dissolution and seepage fillings, spongy dissolution, dissolution fissures and karrens, and atmospheric freshwater cements. It is also concluded that the formation of pore-type reservoirs (including micrite dolomite with moldic pore, grain dolomite and microbialite) is related to the facies-controlled eogenetic karst driven by high-frequency sea level fluctuation, and moderate eogenetic karst has the best improvement to the reservoir quality. With the further increase of karst intensity, the reservoir physical property gradually would become worse.

The Caledonian - early Hercynian weathering crust karst has limited improvement to the reservoirs in the M_5^4-M_5^1 sub-members. Although giving rise to a small number of small karst caves, more importantly, it has superposed reformation and destruction to the pre-existing porous layers, or destructs the lateral continuity of the facies-controlled eogenetic karst reservoir due to formation denudation or erosion. Its biggest contribution is to make the overlying coal measure in direct contact with the facies-controlled eogenetic karst reservoir. Hence, the model of “facies-controlled eogenetic karst controlling reservoirs and weathering crust karst in Caledonian - early Hercynian period controlling hydrocarbon accumulation” has been established.

References

[1] HOU Fanghao, FANG Shaoxian, DONG Zhaoxiong, et al. The developmental characters of sedimentary environments and lithofacies of Middle Ordovician Majiagou Formation in Ordos Basin. Acta Sedimentologica Sinica, 2003, 21(1): 106–112.

[2] MA Zhenfang, ZHOU Shuxun. The weathered paleocrust on the Ordovician in Ordos Basin and its relationship to gas accumulation. Petroleum Exploration and Development, 1999, 26(5): 21–23.

[3] HE Jiang, FANG Shaoxian, HOU Fanghao, et al. Vertical zonation of weathered crust ancient karst and reservoir evaluation and prediction: A case study of $M5_5$–$M5_1$ sub-members of Majiagou Formation in gas fields, central Ordos Basin, NW China. Petroleum Exploration and Development, 2013, 40(5): 534–542.

[4] FANG Shaoxian, HE Jiang, HOU Fanghao, et al. Reservoirs pore space types and evolution in $M5_5$ to $M5_1$ sub-members of Majiagou Formation of Middle Ordovician in central gasfield area of Ordos Basin. Acta Petrologica Sinica, 2009, 25(10): 2425–2441.

[5] LIU Xinshe, XIONG Ying, WEN Caixia, et al. Rock types and sedimentary environment of the $Ma5_{1+2}$ carbonates in Northeastern Ordos Basin. Acta Sedimentologica Sinica, 2016, 34(5): 912–923.

[6] XIAO D, TAN X, ZHANG D, et al. Discovery of syngenetic and eogenetic karsts in the Middle Ordovician gypsum-bearing dolomites of the eastern Ordos Basin (central China) and their heterogeneous impact on reservoir quality. Marine and Petroleum Geology, 2019, 99: 190–207.

[7] XIONG Y, TAN X, ZUO Z, et al. Middle Ordovician multi-stage penecontemporaneous karstification in North China: Implications for reservoir genesis and sea level fluctuations. Journal of Asian Earth Sciences, 2019, 183: 103969.

[8] FENG Zengzhao, BAO Zhidong. Lithofacies paleogeography of Majiagou age of Ordovician in Ordos Basin. Acta Sedimentologica Sinica, 1999, 17(1): 1–8.

[9] FU Jinhua, ZHENG Congbin. Evolution between north China sea and Qilian sea of the Ordovician and the characteristics of lithofacies palaeogeography in Ordos Basin. Journal of Palaeogeography, 2001, 3(4): 25–34.

[10] BURNE R V, MOORE L S. Microbialites: Organosedimentary deposits of benthic microbial communities. Palaios, 1987, 2(3): 241–254.

[11] FLÜGEL E. Microfacies of carbonate rocks: Analysis, interpretation and application. New York: Springer, 2013.

[12] BATHURST R G C. Boring algae, micrite envelopes and lithi-

lithification of molluscan biosparites. Geological Journal, 1966, 5(1): 15–32.

[13] CHEN Jingshan, LI Zhong, WANG Zhenyu, et al. Paleokarstification and reservoir distribution of Ordovician carbonates in Tarim Basin. Acta Sedimentologica Sinica, 2007, 25(6): 858–868.

[14] VACHER H L, MALROIE J E. Eogenetic karst from the perspective of an equivalent porous medium. Carbonates and Evaporites, 2002, 17(2): 182.

[15] ZHANG Baomin, LIU Jingjiang. Classification and characteristics of karst reservoirs in China and related theories. Petroleum Exploration and Development, 2009, 36(2): 12–29.

[16] QIANG Zitong. Carbonate reservoir geology. Dongying: China University of Petroleum Press, 1998.

[17] GRIMES K G. Syngenetic karst in Australia: A review. Helictite, 2006, 39(2): 27–38.

[18] TAN Xiucheng, XIAO Di, CHEN Jingshan, et al. New advance and enlightenment of eogenetic karstification. Journal of Palaeogeography, 2015, 17(4): 441–456.

[19] MOORE P J, MARTIN J B, SCREATON E J, et al. Conduit enlargement in an eogenetic karst aquifer. Journal of Hydrology, 2010, 393(3/4): 143–155.

[20] LONGMAN M W. Carbonate diagenetic textures from near-surface diagenetic environments. AAPG Bulletin, 1980, 64(4): 461–487.

[21] JAMES N P, CHOQUETTE P W. Paleokarst. New York: Springer-Verlag, 1988.

[22] SALLER A H, DICKSON J A D, MATSUDA F. Evolution and distribution of porosity associated with subaerial exposure in upper Paleozoic platform limestones, west Texas. AAPG Bulletin, 1999, 83(11): 1835–1854.

[23] NÉGREL P, ROY S, PETELET-GIRAUD E, et al. Long-term fluxes of dissolved and suspended matter in the Ebro River Basin (Spain). Journal of Hydrology, 2007, 342(3): 249–260.

[24] LIU Z, YUAN D, DREYBRODT W. Comparative study of dissolution rate-determining mechanisms of limestone and dolomite. Environmental Earth Sciences, 2005, 49(2): 274–279.

[25] XIAO D, TAN X, FAN L, et al. Reconstructing large-scale karst paleogeomorphology at the top of the Ordovician in the Ordos Basin, China: Control on natural gas accumulation and paleogeographic implications. Energy Science & Engineering, 2019, 7(6): 3234–3254.

[26] HUANG Difan, XIONG Chuanwu, YANG Junjie, et al. Gas source discrimination and natural gas genetic types of central gas field Ordos Basin, China. Natural Gas Industry, 1996, 16(6): 1–5.

[27] DAI J, LI J, LUO X, et al. Stable carbon isotope compositions and source rock geochemistry of the giant gas accumulations in the Ordos Basin, China. Organic Geochemistry, 2005, 36(12): 1617–1635.

[28] XIA X, CHEN J, BRAUN R, et al. Isotopic reversals with respect to maturity trends due to mixing of primary and secondary products in source rocks. Chemical Geology, 2013, 339: 205–212.

[29] WEI Xinshan, WEI Liubin, REN Junfeng, et al. Differential distribution of natural gas in the Lower Paleozoic paleokarst gas reservoir, Ordos Basin. Natural Gas Geoscience, 2018, 29(2): 178–188.